PERGAMON

International Journal of Solids and Structures 38 (2001) 6925–6940

INTERNATIONAL JOURNAL OF SOLIDS and STRUCTURES

www.elsevier.com/locate/ijsolstr

A comprehensive description for shape memory alloys with a two-phase constitutive model

X. Peng *, Y. Yang, S. Huang

Institute of Intelligent Structures, Chongqing University, Chongqing 400044, People's Republic of China

Received 22 February 2000

Abstract

A comprehensive description for the constitutive behavior of polycrystalline shape memory alloys (SMAs) is proposed based on the concept that a SMA is dynamically composed of austenite and martensite, the constitutive behavior of which is a dynamic combination of the individual behavior of each of the two phases. In the interested ranges of stress and temperature the behavior of austenite is assumed to be linearly elastic while that of martensite elastoplastic. The main features of SMAs such as ferroelasticity at lower temperature, shape memory effect (SME), pseudoelasticity at higher temperature and other typical features can be successfully replicated with the proposed constitutive model. The ferroelasticity, pseudoelasticity and SME of SMA Au–47.5 at.%Cd subjected to uniaxial forward and reverse loading and the pseudoelasticity of Cu–Al–Zn–Mn SMA polycrystal subjected to proportional and nonproportional complex stress or strain histories are analyzed and compared with the experimental results.

Keywords: Shape memory alloys; Two-phase mixture; Ferroelasticity; Pseudoelasticity; Shape memory effect; Constitutive model

1. Introduction

Shape memory alloys (SMAs) are composed of austenite and martensite, the forward and reverse thermoelastic martensitic transformation in which determines the amazing properties of SMAs. When cooled down below a critical temperature, a SMA will mainly be composed of martensite, behave ferroelastically (FE) and easily be manipulated in a very large strain range. When heated over a critical temperature, the SMA changes back to the austenitic phase, the previous inelastic strain recovers and the SMA resumes the shape it normally has at the higher temperature. This is shape memory effect (SME). At higher temperature, applied stress may cause martensitic transformation and a SMA may deform plastically, both of which may recover as the applied stress is removed, which is referred to as pseudoelasticity (PE). These particular properties make SMAs be used as a kind of smart materials and receive increasing attention in recent years.

* Corresponding author. Tel.: +86-23-6510-3597; fax: +86-23-6510-6656.
E-mail address: xhpeng@cqu.edu.cn (X. Peng).

0020-7683/01/$ - see front matter
PII: S0020-7683(00)00402-9

Great progress has been made in the constitutive modeling for SMAs in the past 20 years. In the early constitutive models, attention was mainly paid to the phenomenological description for the behavior under simple tension and compression with thermodynamic approaches or statistical micromechanics, such as those by Falk (1980) and Achenbach et al. (1986). These models could qualitatively explain the pseudoelasticity and SME of SMAs, but it remained problems to be applied in practice. Graesser and Cozzarelli (1991) phenomenologically proposed a simple and practical model by introducing an error function into the back stress, which was further extended to the case of general state of stress (Graesser and Cozzarelli, 1994). Tanaka (1986) obtained an expression for stress rate by making use of thermodynamic laws, which was then simplified and integrated by Liang and Rogers (1990) to express the stress as a function of strain, temperature and the volume fraction of martensite. Boyd (1994) proposed a model by decomposing strain into three parts corresponding respectively to elasticity, temperature and phase transformation, which could describe the pseudoelasticity and SME of SMAs and was applied to the analysis of intelligent structures. Liang's and Boyd's models did not involve plastic strain, which plays a very substantial role in both pseudoelastic behavior and SME. A constitutive model based on an internal variable formalism and the framework of generalized plasticity was proposed by Auricchio et al. (1997), with which the basic features of SMAs could be reproduced. Levitas (1995) discussed the phase transitions in elastoplastic materials and the corresponding conditions. It was suggested that the phase transformation in a microregion be related to a critical value of the Gibbs free energy, and a description for the phase transformation in polycrystalline SMAs was obtained with a statistical method (Fischer et al., 1997). Goo and Lexcellent (1997) proposed a micromechanically based Helmoholtz free energy, based on which a kinetic relationship, a martensitic nucleation criterion and the reorientation criterion of martensitic variants were obtained.

Being cognizant that the complex constitutive behavior of SMAs could hardly be well described with phenomenological models, Tanaka et al. (1986) and Patoor et al. (1988) investigated the constitutive behavior of SMAs through microscopic analysis and the corresponding averaging procedure. It was, however, limited to stress induced forward martensitic transformation and could not work well in the cases involving reverse martensitic transformation and nonproportional loading. A micro–macro thermomechanical modelization of the grain behavior was proposed by Siredey et al. (1999), in which an average martensite fraction in each domain was used as an internal variable, and a description for the evolution of the material was suggested. The overall behavior of polycrystalline SMAs was then obtained with a self-consistent scheme. Sun and Hwang (1993) proposed a model by making use of micromechanics and thermodynamics, which could describe both forward and reverse martensitic transformation and the main features of SMAs under complex deformation and temperature histories. These models, however, are complicated and remain problems in practical engineering application.

The constitutive behavior of SMAs strongly depends on the histories of temperature and stress, and the resulting forward and reverse thermoelastic martensitic transformation. A two-phase constitutive model for SMAs is proposed based on the concept that a SMA is dynamically composed of austenite and martensite, and the constitutive behavior of the SMA is substantially the dynamic combination of that of each of the two phases. Within the interested ranges of stress and temperature, the behavior of austenite is assumed linearly elastic while that of martensite elastoplastic. The developed constitutive model can comprehensively describe the constitutive behavior of SMAs subjected to complex thermomechanical loading histories. The forward and reverse martensitic transformation, SME, ferroelasticity and pseudoelasticity of SMA Au–47.5 at.%Cd and the response of pseudoelastic behavior of Cu–Al–Zn–Mn SMA polycrystal subjected to biaxially nonproportional stress or strain histories are described. The satisfactory agreement between the analytical and experimental results (Sittner et al., 1995; Sittner and Takuda, 1995) well demonstrates the validity of the proposed constitutive model.

The proposed model separates the complicated constitutive behavior of a SMA into the simple responses of its two phases, and provides an easy but comprehensive method for the description for the constitutive

behavior of SMAs under complex thermomechanical loading. Compared with the existing constitutive models, the proposed one is concise and can easily be applied in practice.

2. A two-phase constitutive model for SMAs

A SMA is composed of austenite and martensite and the volume fraction of each phase evolves during a thermomechanical loading process. A SMA behaves ferroelastically at lower level of stress or temperature when it is mainly composed of martensite, but it behaves almost elastically at higher level of stress or temperature when it is mainly composed of austenite. The macroscopic behavior of the SMA, such as ferroelasticity, pseudoelasticity and SME can generally be regarded as the combination of the individual behavior of each of the two phases.

In the following, the discussion is restricted to the case of small deformation, the material is assumed plastically incompressible and the transformation lattice volume change is neglected (Sun and Hwang, 1993). The deviatoric strain $\mathbf{e}$ can, in general, be assumed to consist of elastic component $\mathbf{e}^{\mathrm{e}}$, plastic component $\mathbf{e}^{\mathrm{p}}$ and phase transformation strain $\mathbf{e}^{\mathrm{T}}$, i.e.,

$$\mathbf{e} = \mathbf{e}^{\mathrm{e}} + \mathbf{e}^{\mathrm{p}} + \mathbf{e}^{\mathrm{T}}, \tag{1}$$

where $\mathbf{e}^{\mathrm{T}}$ is related to the temperature induced recovery of inelastic distortion. Assuming the strains in both martensite and austenite are identical to the overall strain in the SMA, the macroscopic deviatoric stress $\mathbf{s}$ and volumetric stress σ_{kk} of SMAs can be expressed as follows

$$\mathbf{s} = \bar{\mathbf{s}}_{\mathrm{A}} + \bar{\mathbf{s}}_{\mathrm{M}}, \quad \sigma_{kk} = (\overline{\sigma}_{kk})_{\mathrm{A}} + (\overline{\sigma}_{kk})_{\mathrm{M}}, \tag{2}$$

in which $\bar{\mathbf{s}}_{\mathrm{A}}$, $(\overline{\sigma}_{kk})_{\mathrm{A}}$ and $\bar{\mathbf{s}}_{\mathrm{M}}$, $(\overline{\sigma}_{kk})_{\mathrm{M}}$ denote respectively the contributions of austenite and martensite to the corresponding overall stress components.

It should be noted that the adoption of Eq. (2) is based on the following consideration. Macroscopically speaking, there is no distinct structure in a polycrystalline SMA that definitely indicates the relationship between the stresses (or strains) in a SMA and its two phases. On the other hand, for a given strain the stress response in the martensite is, in general, much lower than that in the austenite, and the stress in the SMA usually lies between those in its two phases. Eq. (2), together with the description for forward and reverse martensitic transformation, may therefore provides a simpler way to obtain the overall stress response of a SMA.

With experimental observation it is acceptable to assume that the austenite is elastic while the martensite elastoplastic within the interested ranges of stress and temperature. Letting ξ_{A} and ξ denote respectively the volume fractions of austenite and martensite, $\mathbf{s}_{\mathrm{M}}$ and $(\sigma_{kk})_{\mathrm{M}}$ denote respectively the deviatoric and the volumetric stress components of martensite, $\mathbf{s}_{\mathrm{A}}$ and $(\sigma_{kk})_{\mathrm{A}}$ denote those of austenite, and keeping in mind the assumption that the strain and the phase transformation strain in martensite and austenite are identical to the overall $\mathbf{e}$ and $\mathbf{e}^{\mathrm{T}}$, the conventional mixture theory gives

$$\begin{aligned} &\bar{\mathbf{s}}_{\mathrm{M}} = \xi \mathbf{s}_{\mathrm{M}}, \quad (\overline{\sigma}_{kk})_{\mathrm{M}} = \xi (\sigma_{kk})_{\mathrm{M}} \\ &\bar{\mathbf{s}}_{\mathrm{A}} = \xi_{\mathrm{A}} \mathbf{s}_{\mathrm{A}}, \quad (\overline{\sigma}_{kk})_{\mathrm{A}} = \xi_{\mathrm{A}} (\sigma_{kk})_{\mathrm{A}}, \end{aligned} \tag{3}$$

with

$$\xi + \xi_{\mathrm{A}} = 1. \tag{4}$$

It may be more complicated for SMAs when the dynamic change of volume fraction and the effect of boundaries between grains and phases are taken into account. In order to make the model more general, the deviatoric part in Eq. (3) is rewritten in a more general form as follows

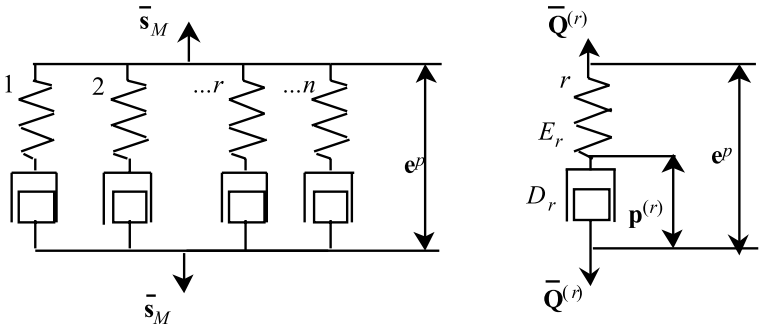

Fig. 1. Mechanical model for the contribution of martensite.

$$\bar{\mathbf{s}}_{\mathrm{A}} = \bar{\mathbf{s}}_{\mathrm{A}}(\mathbf{e}, \mathbf{e}^{\mathrm{T}}, T, \xi), \qquad \bar{\mathbf{s}}_{\mathrm{M}} = \bar{\mathbf{s}}_{\mathrm{M}}(\mathbf{e}, \mathbf{e}^{\mathrm{T}}, T, \mathbf{p}^{(r)}, \xi), \tag{5}$$

where T denotes temperature, $\mathbf{p}^{(r)}$ $(r = 1, 2, \ldots, n)$ represents a set of internal variables related to irreversible deformation. It is assumed in Eq. (5) that the contribution of austenite is determined by the current states of strain and the phase transformation strain, temperature and martensitic volume fraction, while besides these, an additional set of internal variables $\mathbf{p}^{(r)}$ $(r = 1, 2, \ldots, n)$ were introduced to describe the constitutive behavior of martensite.

Iwan (1967) used a simple mechanical model consisting of elastic and plastic elements to describe the elastoplastic behavior of materials. It was extended to the model shown in Fig. 1 for the description of the elastoplastic behavior of martensite. It contains a series of parallel Maxwell-type elements and an additional spring in series. In Fig. 1, the rth dissipation mechanism is described by a spring E_r (with macroscopically average stiffness $\overline{C}_r$) and a dashpot-like block D_r (with macroscopically average plastic damping coefficient $\overline{a}_r$). E_r is related to the stochastic internal structures and the energy stored in E_r corresponds to that stored in the microstress fields induced by the respective pattern of defects at the microlevel. $\mathbf{e}^{\mathrm{p}}$ denotes plastic strain component. $\overline{\mathbf{Q}}^{(r)}$ is the generalized force conjugated with the rth internal variable $\mathbf{p}^{(r)}$ and the following inequality should be satisfied if any change occurs to $\mathbf{p}^{(r)}$ (Fan and Peng, 1991; Peng and Ponter, 1994)

$$\overline{\mathbf{Q}}^{(r)} : \mathrm{d}\mathbf{p}^{(r)} \geqslant 0 \quad (r = 1, 2, \ldots, n). \tag{6}$$

From Fig. 1, one obtains

$$\bar{\mathbf{s}}_{\mathrm{M}} = \sum_{r=1}^{n} \overline{\mathbf{Q}}^{(r)}, \tag{7}$$

in which $\overline{\mathbf{Q}}^{(r)}$ is assumed to relate the response of the E_r and the flow of D_r with the following phenomenological relationships,

$$\overline{\mathbf{Q}}^{(r)} = \overline{C}_r(T, \xi)(\mathbf{e}^{\mathrm{p}} - \mathbf{p}^{(r)}), \qquad \overline{\mathbf{Q}}^{(r)} = \overline{a}_r(T, \xi)\, \frac{\mathrm{d}\mathbf{p}^{(r)}}{\mathrm{d}z}, \tag{8}$$

where z is generalized time. It was observed by Sittner et al. (1995) in biaxial tension–torsion tests that for some SMAs the response is not isotropic and the equivalent stress does not obey the von Mises rule. This phenomenon can be described by introducing the following defined generalized time

$$\mathrm{d}z = \frac{\mathrm{d}\varsigma}{f(z)}, \quad (\mathrm{d}\varsigma)^2 = \mathrm{d}\mathbf{e}^{\mathrm{p}} : \mathbf{P} : \mathrm{d}\mathbf{e}^{\mathrm{p}}, \tag{9}$$

where $\mathbf{P}$ is a material-dependent tensor of rank four and $f(z)$ describes the change of the plastic damping property of the dashpot-like blocks D_r (see Fig. 1). Differentiating Eq. (8) leads to

$$\mathrm{d}\overline{\mathbf{Q}}^{(r)} = \overline{C}_r(T,\xi)\,\mathrm{d}\mathbf{e}^{\mathrm{p}} + \left(\frac{1}{\overline{C}_r}\frac{\partial \overline{C}_r}{\partial T}\,\mathrm{d}T + \frac{1}{\overline{C}_r}\frac{\partial \overline{C}_r}{\partial \xi}\,\mathrm{d}\xi - \alpha_r\,\mathrm{d}z\right)\overline{\mathbf{Q}}^{(r)}, \tag{10}$$

where

$$\alpha_r = \frac{\overline{C}_r}{\overline{a}_r}.$$

Substituting Eq. (10) into Eq. (7) yields

$$\mathrm{d}\bar{\mathbf{s}}_{\mathrm{M}} = \sum_{r=1}^{n}\mathrm{d}\overline{\mathbf{Q}}^{(r)} = \overline{A}\,\mathrm{d}\mathbf{e}^{\mathrm{p}} + \overline{\mathbf{B}}\,\mathrm{d}z + \overline{\mathbf{C}}\,\mathrm{d}T + \overline{\mathbf{D}}\,\mathrm{d}\xi, \tag{11}$$

in which

$$\overline{A} = \sum_{r=1}^{n}\overline{C}_r, \quad \overline{\mathbf{B}} = -\sum_{r=1}^{n}\alpha_r\overline{\mathbf{Q}}^{(r)}, \quad \overline{\mathbf{C}} = \sum_{r=1}^{n}\frac{1}{\overline{C}_r}\frac{\partial \overline{C}_r}{\partial T}\overline{\mathbf{Q}}^{(r)}, \quad \overline{\mathbf{D}} = \sum_{r=1}^{n}\frac{1}{\overline{C}_r}\frac{\partial \overline{C}_r}{\partial \xi}\overline{\mathbf{Q}}^{(r)}. \tag{12}$$

If $\overline{C}_1$ tends to infinite, it is easily seen in Fig. 1 that $\mathbf{p}^{(1)} = \mathbf{e}^{\mathrm{p}}$ and making use of Eq. (8), Eq. (7) can be rewritten as

$$\bar{\mathbf{s}}_{\mathrm{M}} - \bar{\mathbf{r}} = \overline{a}_1\frac{\mathrm{d}\mathbf{e}^{\mathrm{p}}}{\mathrm{d}z}, \tag{13}$$

where

$$\bar{\mathbf{r}} = \sum_{r=2}^{n}\overline{\mathbf{Q}}^{(r)}. \tag{14}$$

The combination of Eq. (13) and Eq. (9) gives

$$(\bar{\mathbf{s}}_{\mathrm{M}} - \bar{\mathbf{r}}) : \mathbf{P} : (\bar{\mathbf{s}}_{\mathrm{M}} - \bar{\mathbf{r}}) = [\overline{a}_1 f(z)]^2. \tag{15}$$

Eqs. (15) and (13) have the forms of yield surface and flow rule, in which $\bar{\mathbf{r}}$ can be regarded as the center and $\mathbf{P}$ determines the shape of the surface.

It is known that the temperature induced reverse martensitic transformation causes the recovery of the distortion of lattice, which is related to both the current states of plastic strain and martensitic phase transformation strain. The temperature induced change of martensite volume fraction during reverse martensitic transformation. Letting $\boldsymbol{\eta} = \mathbf{e}^{\mathrm{p}} + \mathbf{e}^{\mathrm{T}}$, $\mathrm{d}\mathbf{e}^{\mathrm{T}}$ can be assumed to take the following linear relation

$$\mathrm{d}\mathbf{e}^{\mathrm{T}} = \frac{1}{2}k_T\boldsymbol{\eta}\left(\frac{\partial \xi}{\partial T}\,\mathrm{d}T - \left|\frac{\partial \xi}{\partial T}\mathrm{d}T\right|\right), \tag{16}$$

where k_T is a material constant. It is seen that $\mathbf{e}^{\mathrm{T}}$ changes only when both $\boldsymbol{\eta} \neq 0$ and $(\partial\xi/\partial T)\,\mathrm{d}T < 0$, i.e., reverse martensitic transformation occurs.

The elastic response of martensite and austenite can be expressed, by making use of Eq. (1) and keeping in mind that austenite is assumed elastic, as

$$\bar{\mathbf{s}}_{\mathrm{M}} = 2\overline{G}_{\mathrm{M}}(T,\xi)(\mathbf{e} - \mathbf{e}^{\mathrm{p}} - \mathbf{e}^{\mathrm{T}}), \qquad \bar{\mathbf{s}}_{\mathrm{A}} = 2\overline{G}_{\mathrm{A}}(T,\xi)(\mathbf{e} - \mathbf{e}^{\mathrm{T}}), \tag{17}$$

where $\overline{G}_{\mathrm{M}}$ and $\overline{G}_{\mathrm{A}}$ are respectively the macroscopic average shear modulus of martensite and austenite. The differential of Eq. (17) can be derived as,

$$\begin{aligned} \mathrm{d}\overline{\mathbf{s}}_{\mathrm{M}} &= 2\overline{G}_{\mathrm{M}}(\mathrm{d}\mathbf{e} - \mathrm{d}\mathbf{e}^{\mathrm{p}} - \mathrm{d}\mathbf{e}^{\mathrm{T}}) + \frac{\overline{\mathbf{s}}_{\mathrm{M}}}{\overline{G}_{\mathrm{M}}}\left(\frac{\partial \overline{G}_{\mathrm{M}}}{\partial T}\mathrm{d}T + \frac{\partial \overline{G}_{\mathrm{M}}}{\partial \xi}\mathrm{d}\xi\right), \\ \mathrm{d}\overline{\mathbf{s}}_{\mathrm{A}} &= 2\overline{G}_{\mathrm{A}}(\mathrm{d}\mathbf{e} - \mathrm{d}\mathbf{e}^{\mathrm{T}}) + \frac{\overline{\mathbf{s}}_{\mathrm{A}}}{\overline{G}_{\mathrm{A}}}\left(\frac{\partial \overline{G}_{\mathrm{A}}}{\partial T}\mathrm{d}T + \frac{\partial \overline{G}_{\mathrm{A}}}{\partial \xi}\mathrm{d}\xi\right). \end{aligned} \tag{18}$$

For simplicity, the transformation lattice volume change is neglected in the present stage since for most SMAs it is negligible compared with the lattice shear deformation (Sun and Hwang, 1993). The contributions of martensite and austenite to the overall volumetric stress can, therefore, be determined respectively with

$$\begin{aligned} (\overline{\sigma}_{kk})_{\mathrm{M}} &= 3\overline{K}_{\mathrm{M}}(T,\xi)[\varepsilon_{kk} - 3\alpha_{\mathrm{M}}(T)(T - T_0)], \\ (\overline{\sigma}_{kk})_{\mathrm{A}} &= 3\overline{K}_{\mathrm{A}}(T,\xi)[\varepsilon_{kk} - 3\alpha_{\mathrm{A}}(T)(T - T_0)], \end{aligned} \tag{19}$$

where T_0 denotes reference temperature, ε_{kk} the volumetric strain, $\overline{K}_{\mathrm{M}}$ and α_{M} the macroscopic average elastic volumetric modulus and the thermal expansion coefficient of martensite, respectively. The differential of Eq. (19) is

$$\begin{aligned} (\mathrm{d}\overline{\sigma}_{kk})_{\mathrm{M}} &= 3\overline{K}_{\mathrm{M}}(T,\xi)\,\mathrm{d}\varepsilon_{kk} + \frac{1}{\overline{K}_{\mathrm{M}}}\frac{\partial \overline{K}_{\mathrm{M}}}{\partial \xi}(\overline{\sigma}_{kk})_{\mathrm{M}}\,\mathrm{d}\xi \\ &\quad + \left[\frac{1}{\overline{K}_{\mathrm{M}}}\frac{\partial \overline{K}_{\mathrm{M}}}{\partial T}(\overline{\sigma}_{kk})_{\mathrm{M}} - 9\frac{\mathrm{d}\alpha_{\mathrm{M}}}{\mathrm{d}T}\overline{K}_{\mathrm{M}}(T - T_0) - 9\alpha_{\mathrm{M}}(T)\overline{K}_{\mathrm{M}}\right]\mathrm{d}T, \\ (\mathrm{d}\overline{\sigma}_{kk})_{\mathrm{A}} &= 3\overline{K}_{\mathrm{A}}(T,\xi)\,\mathrm{d}\varepsilon_{kk} + \frac{1}{\overline{K}_{\mathrm{A}}}\frac{\partial \overline{K}_{\mathrm{M}}}{\partial \xi}(\overline{\sigma}_{kk})_{\mathrm{A}}\,\mathrm{d}\xi \\ &\quad + \left[\frac{1}{\overline{K}_{\mathrm{A}}}\frac{\partial \overline{K}_{\mathrm{A}}}{\partial T}(\overline{\sigma}_{kk})_{\mathrm{A}} - 9\frac{\mathrm{d}\alpha_{\mathrm{A}}}{\mathrm{d}T}\overline{K}_{\mathrm{A}}(T - T_0) - 9\alpha_{\mathrm{A}}(T)\overline{K}_{\mathrm{A}}\right]\mathrm{d}T. \end{aligned} \tag{20}$$

In a stress-free state the volume fraction of martensite is determined by temperature, and applied stress may increase the transformation temperature. Tanaka (1986), therefore, suggested the following relation for the determination of the volume fraction ξ,

$$\xi = \begin{cases} 1 - \exp[-A_{\mathrm{m}}\langle M_{\mathrm{s}} + B_{\mathrm{m}}\sigma_{\mathrm{e}} - T\rangle] & A \to M \\ \exp[-A_{\mathrm{a}}\langle T - (A_{\mathrm{s}} + B_{\mathrm{a}}\sigma_{\mathrm{e}})\rangle] & M \to A, \end{cases} \tag{21}$$

in which

$$\langle \Phi \rangle = \begin{cases} \Phi & \text{if } \Phi > 0 \\ 0 & \text{if } \Phi \leqslant 0, \end{cases} \tag{22}$$

M_{s} and A_{s} denote respectively start temperatures of martensitic and austenitic transformation, A_{m}, B_{m}, A_{a} and B_{a} material constants related to phase transformation processes, and σ_{e} is equivalent stress defined by

$$\sigma_{\mathrm{e}} = \sqrt{\frac{3}{2}\mathbf{s} : \mathbf{P} : \mathbf{s}}. \tag{23}$$

σ_{e} is reduced to the conventional equivalent stress if $\mathbf{P}$ is chosen an identity tensor.

3. Analytical approach

3.1. Specification of the constitutive model

For simplicity in the initial application, it is assumed that

$$\overline{G}_{\mathrm{A}}(T,\xi) = (1-\xi)g_{\mathrm{A}}(T)G^0_{\mathrm{A}}, \qquad \overline{K}_{\mathrm{A}}(T,\xi) = (1-\xi)g_{\mathrm{A}}(T)K^0_{\mathrm{A}}, \tag{24}$$

$$\begin{aligned} &\overline{C}_r(T,\xi) = \xi g_{\mathrm{M}}(T)C^0_r, \qquad \overline{a}_r(T,\xi) = \xi g_{\mathrm{M}}(T)a^0_r, \\ &\overline{G}_{\mathrm{M}}(T,\xi) = \xi g_{\mathrm{M}}(T)\,G^0_{\mathrm{M}}, \qquad \overline{K}_{\mathrm{M}}(T,\xi) = \xi g_{\mathrm{M}}(T)K^0_{\mathrm{M}}, \end{aligned} \tag{25}$$

where G^0_{A} and K^0_{A} are respectively the elastic shear and volumetric moduli of austenite at reference temperature T_0, G^0_{M} and K^0_{M} are those of martensite, $g_{\mathrm{A}}(T)$ and $g_{\mathrm{M}}(T)$ are temperature-dependent coefficients of austenite and martensite, respectively, C^0_r and a^0_r are the parameters of plasticity of martensite at T_0. With these definitions one obtains the expressions shown in Eq. (3), in which

$$\mathbf{s}_{\mathrm{A}} = 2g_{\mathrm{A}}(T)G^0_{\mathrm{A}}(\mathbf{e}-\mathbf{e}^{\mathrm{T}}), \qquad (\sigma_{kk})_{\mathrm{A}} = 3g_{\mathrm{A}}(T)K^0_{\mathrm{A}}[\varepsilon_{kk} - 3\alpha_{\mathrm{A}}(T-T_0)] \tag{26}$$

denote respectively the deviatoric and the volumetric components of the stress in austenite, and

$$\mathbf{s}_{\mathrm{M}} = 2g_{\mathrm{M}}(T)G^0_{\mathrm{M}}(\mathbf{e}-\mathbf{e}^{\mathrm{p}}-\mathbf{e}^{\mathrm{T}}), \qquad (\sigma_{kk})_{\mathrm{M}} = 3g_{\mathrm{M}}(T)K^0_{\mathrm{M}}[\varepsilon_{kk} - 3\alpha_{\mathrm{M}}(T-T_0)] \tag{27}$$

denote those in martensite. Alternatively one can derive

$$\mathbf{s}_{\mathrm{M}} = \sum_{r=1}^{n}\mathbf{Q}^{(r)} \tag{28}$$

$$\mathbf{Q}^{(r)} = C_r(T)\,(\mathbf{e}^{\mathrm{p}} - \mathbf{p}^{(r)}) = C_r(T)\frac{\mathrm{d}\mathbf{p}^{(r)}}{\mathrm{d}z} \tag{29}$$

and Eqs. (13)–(15) can then be rewritten as

$$\mathbf{s}_{\mathrm{M}} - \mathbf{r} = a_1\frac{\mathrm{d}\mathbf{e}^{\mathrm{p}}}{\mathrm{d}z}, \quad (\mathbf{s}_{\mathrm{M}} - \mathbf{r}) : \mathbf{P} : (\mathbf{s}_{\mathrm{M}} - \mathbf{r}) = [a_1 f(z)]^2, \tag{30}$$

in which

$$\mathbf{r} = \sum_{r=2}^{n}\mathbf{Q}^{(r)}. \tag{31}$$

Eq. (30) represents the yield condition and flow rule of martensite, in which a_1 represents the initial yield stress of martensite.

3.2. Identification of the material parameters

The involved material parameters can be separated into three groups: parameters of martensite, those of austenite and parameters related to forward and reverse martensitic transformation. These material parameters can be identified by the following procedure:

- Keeping temperature sufficiently low ($T < M_f$) so that the SMA to be tested is composed of pure martensite, the following parameters can be identified with a simple elastoplastic deformation test:
  (1) Young's modulus E_M (or shear modulus G_M) and Poisson's ratio v_M
  (2) Plastic parameters C_r and α_r $(r = 1, \ldots, n)$
  (3) Hardening parameter $f(z)$
  (4) **P**, if the response is anisotropic
  (5) Adjusting temperature and repeating (1) or (2) several times; then determining $g_M(T)$ using the obtained set of G_M or C_r.
- Keeping temperature sufficiently high so that no martensitic transformation can occur when applying the stress on the SMA to be tested and the SMA is composed of pure austenite during testing, the following parameters can be identified with a simple test:
  (1) Young's modulus E_A (or shear modulus G_A) and Poisson's ratio v_A
  (2) Adjusting temperature and repeating (1) several times; then determining $g_A(T)$ using the obtained set of G_A.
- M_f, M_s, A_s, A_f are usually provided by material provider, and the rest parameters related to forward and reverse martensitic transformation can be identified by using pseudoelasticity and SME:
  (1) A_m, B_m, in a loading process involving stress induced martensitic transformation
  (2) A_a, B_a, in the subsequent unloading process involving stress induced reverse martensitic transformation
  (3) k_T with a SME (temperature induced reverse martensitic transformation that induces the recovery of previous residual strain).

3.3. Numerical algorithm

It is not intended to introduce a yield surface in the following analysis.

In order to analyze the response of the SMA subjected to given temperature and strain histories, the following governing equation can be obtained by combining Eqs. (11) and (18)

$$(\overline{A} + 2\overline{G}_M)\,\mathrm{d}\mathbf{e}^p = -\overline{\mathbf{B}}\,\mathrm{d}z + \mathrm{d}\overline{\psi}, \tag{32}$$

where

$$\mathrm{d}\overline{\psi} = 2\overline{G}_M(\mathrm{d}\mathbf{e} - \mathrm{d}\mathbf{e}^T) - \left(\overline{\mathbf{C}} - \frac{\overline{\mathbf{s}}_M}{\overline{G}_M}\frac{\partial \overline{G}_M}{\partial T}\right)\mathrm{d}T - \left(\overline{\mathbf{D}} - \frac{\overline{\mathbf{s}}_M}{\overline{G}_M}\frac{\partial \overline{G}_M}{\partial \xi}\right)\mathrm{d}\xi. \tag{33}$$

Substituting Eq. (32) into Eq. (9) yields

$$[\overline{\mathbf{B}} : \mathbf{P} : \overline{\mathbf{B}} - (\overline{A} + 2\overline{G}_M)^2 f^2]\,\mathrm{d}z^2 - 2\overline{\mathbf{B}} : \mathbf{P} : \mathrm{d}\overline{\psi}\,\mathrm{d}z + \delta\overline{\psi} : \mathbf{P} : \mathrm{d}\overline{\psi} = 0. \tag{34}$$

Given strain and temperature increments, $\mathrm{d}\xi$ and $\mathrm{d}\mathbf{e}^T$ can be calculated respectively with Eqs. (21) and (16), $\mathrm{d}z$ can be obtained by solving Eq. (34), and then $\mathrm{d}\mathbf{e}^p$ with Eq. (32), $\mathrm{d}\overline{\mathbf{s}}_M$ with Eq. (11) and then $\overline{\mathbf{s}}_M$; on the other hand, $\overline{\mathbf{s}}_A$ can simply be calculated with Eqs. (24) and (3); the overall stress **s** can be calculated with Eq. (2).

If a loading process is temperature- and stress-controlled, the corresponding governing equation can be derived by combining Eqs. (11) and (18) and the differential form of Eq. (24) (first part) as follows

$$\mathrm{d}\mathbf{s} = A\,\mathrm{d}\mathbf{e}^p + \mathbf{B}\,\mathrm{d}z + \mathrm{d}\mathbf{C}, \tag{35}$$

where

$$A = \lambda\overline{A} + 2(\lambda - 1)\overline{G}_M, \quad \mathbf{B} = \lambda\overline{\mathbf{B}}, \tag{36a}$$

$$\mathrm{d}\mathbf{C} = \left[\lambda\left(\overline{\mathbf{C}} - \frac{\bar{\mathbf{s}}_{\mathrm{M}}}{\overline{G}_{\mathrm{M}}}\frac{\partial \overline{G}_{\mathrm{M}}}{\partial T}\right) + \left(\frac{\bar{\mathbf{s}}_{\mathrm{M}}}{\overline{G}_{\mathrm{M}}}\frac{\partial \overline{G}_{\mathrm{M}}}{\partial T} + \frac{\bar{\mathbf{s}}_{\mathrm{A}}}{\overline{G}_{\mathrm{A}}}\frac{\partial \overline{G}_{\mathrm{A}}}{\partial T}\right)\right]\mathrm{d}T + \left[\lambda\left(\overline{\mathbf{D}} - \frac{\bar{\mathbf{s}}_{\mathrm{M}}}{\overline{G}_{\mathrm{M}}}\frac{\partial \overline{G}_{\mathrm{M}}}{\partial \xi}\right) + \left(\frac{\bar{\mathbf{s}}_{\mathrm{M}}}{\overline{G}_{\mathrm{M}}}\frac{\partial \overline{G}_{\mathrm{M}}}{\partial \xi} + \frac{\bar{\mathbf{s}}_{\mathrm{A}}}{\overline{G}_{\mathrm{A}}}\frac{\partial \overline{G}_{\mathrm{A}}}{\partial \xi}\right)\right]\mathrm{d}\xi, \tag{36b}$$

$$\lambda = 1 + \frac{\overline{G}_{\mathrm{A}}}{\overline{G}_{\mathrm{M}}}. \tag{37}$$

Rewriting Eq. (35) as

$$A\,\mathrm{d}\mathbf{e}^{\mathrm{p}} = -\mathbf{B}\,\mathrm{d}z + (\mathrm{d}\mathbf{s} - \mathrm{d}\mathbf{C}) \tag{38}$$

one easily obtains the following equation by using Eq. (9)

$$(\mathbf{B}:\mathbf{P}:\mathbf{B} - A^2 f^2)(\mathrm{d}z)^2 - 2\mathbf{B}:\mathbf{P}:(\mathrm{d}\mathbf{s} - \mathrm{d}\mathbf{C})\,\mathrm{d}z + (\mathrm{d}\mathbf{s} - \mathrm{d}\mathbf{C}):\mathbf{P}:(\mathrm{d}\mathbf{s} - \mathrm{d}\mathbf{C}) = 0. \tag{39}$$

Given stress and temperature increments, $\mathrm{d}\xi$ and $\mathrm{d}\mathbf{e}^{\mathrm{T}}$ can be calculated respectively with Eqs. (21) and (16), $\mathrm{d}z$ from Eq. (39), and then $\mathrm{d}\mathbf{e}^{\mathrm{p}}$ with Eq. (38), and $\mathrm{d}\mathbf{e}$ with Eq. (18).

4. Comprehensive description of the behavior of SMA Au–47.5 at.%Cd

Nakanishi et al. (1973) made a detailed investigation on the uniaxial behavior of SMA Au–47.5 at.%Cd. The main constitutive behavior of the material will be described with the proposed constitutive model.

It is found from the experimental results that the effect of temperature on material constants can be neglected, i.e., $g_{\mathrm{M}} = g_{\mathrm{A}} = 1$. In Eqs. (7) and (11), $n = 3$ is selected to satisfy the requirement of both the accuracy and efficiency in the analysis for practical engineering problems (Valanis and Fan, 1983), and $f(z) = 1$ for the material did not show marked isotropic hardening. M_{s} and A_{s} were given 331 and 345 K (Nakanishi et al., 1973), respectively. For the description of uniaxial constitutive behavior, $\mathbf{P}$ can be taken as an identity tensor. The other material constants were identified as follows:

$$G^0_{\mathrm{M}} = G^0_{\mathrm{M}} = 1500\ \mathrm{MPa}, \quad \nu_{\mathrm{M}} = \nu_{\mathrm{A}} = 0.28,$$
$$C^0_{1,2,3} = 185, 1.8, 0.41\ \mathrm{GPa}, \quad \alpha_{1,2,3} = 30\,000, 840, 65,$$
$$A_{\mathrm{a}}, B_{\mathrm{a}}, A_{\mathrm{m}}, B_{\mathrm{m}} = 0.45, 3.2, 0.25, 4.7, \quad k_T = 3.2.$$

Fig. 2 shows the description of the SME of Au–47.5 at%Cd. In Fig. 2(a) the SMA was stretched at 14°C (287 K) up to $\sigma = 17.2$ MPa and then unloading. It is seen that elastoplastic deformation occurred to the material and large residual strain existed after unloading. Under the given temperature and loading condition, the material kept martensitic during this process. Then the material was heated and the variation of strain against temperature is plotted in Fig. 2(b). It can be seen that the strain almost kept unchanged before the temperature reached A_{s} (345 K) but recovered quickly once temperature exceeded this criterion when reverse martensitic transformation took place. The residual strain gradually tended to vanish when temperature was sufficiently high and the material was mainly composed of austenite. Then if the temperature fell below M_{s}, martensitic transformation would occur and the material would return to its original state. This process can be quite satisfactorily described with the proposed constitutive model.

Fig. 3(a) and (b) shows respectively the tensile/compressive curve and the contributions of austenite and martensite of Au–47.5 at%Cd at 84°C (357 K). It can be seen from Fig. 3(a) that although the two phases were assumed respectively elastic and elastoplastic, the contributions of the two phases $\overline{\sigma}_{\mathrm{A}}$ and $\overline{\sigma}_{\mathrm{M}}$, in which the dynamic change of volume fraction is taken into account, to the overall stress looks like "pseudoelasticity". As the sum of $\overline{\sigma}_{\mathrm{A}}$ and $\overline{\sigma}_{\mathrm{M}}$, the overall stress, therefore, is typically pseudoelastic. It is known that

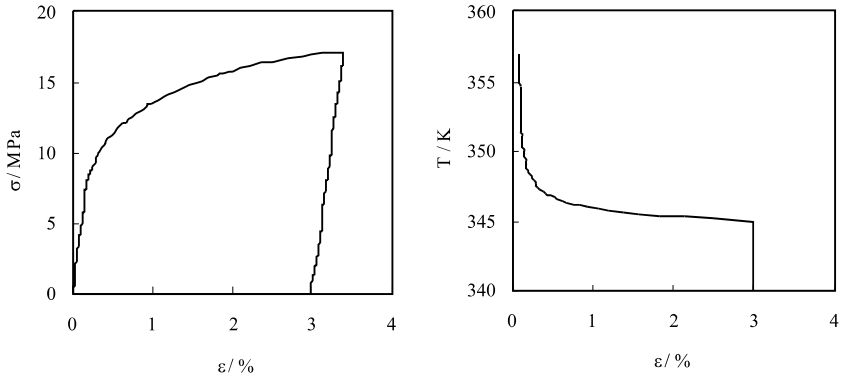

Fig. 2. Analysis for SME of SMA Au–47.5 at%Cd: (a) loading and unloading curve and (b) strain recovery during heating.

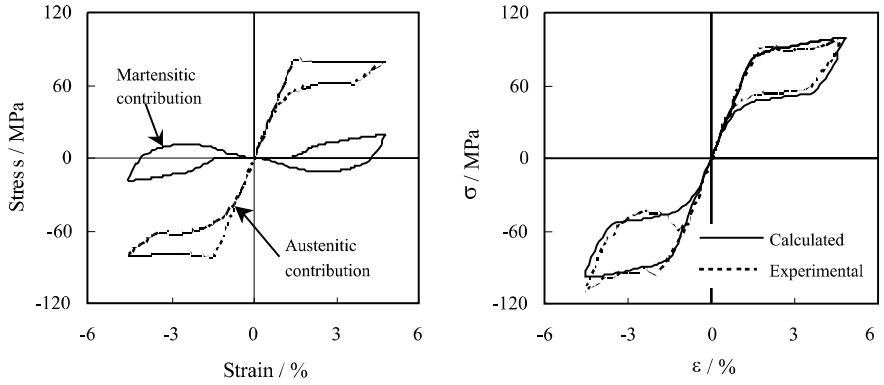

Fig. 3. Pseudoelasticity of Au–47.5 at%Cd at 84°C (357 K) under reversed strain: (a) variations of $\bar{\sigma}_M$ and $\bar{\sigma}_A$ and (b) macroscopic σ–ε curve.

the material was almost composed of austenite at given temperature ($T \approx A_f = 358$ K), applied stress raised $M_s + B_m\sigma_e$, and martensitic transformation took place as $M_s + B_m\sigma_e > T$. During unloading, $A_s + B_a\sigma_e$ decreased and reverse martensitic transformation occurred as $A_s + B_a\sigma_e < T$. Compared with experimental results (Nakanishi et al., 1973), it can be seen that the pseudoelastic behavior was well described with the proposed model.

The tensile/compressive curves of Au–47.5 at.%Cd at different temperatures are shown in Fig. 4(a). At 57°C (330 K) the constitutive behavior was typically elastoplastic. It is known that at this temperature ($T < A_s < A_s + B_a\sigma_e$), the material kept mainly martensitic during the loading and unloading process, and the behavior of the SMA was, in fact, the elastoplastic behavior of martensite. At 93°C (366 K) the material was mainly composed of austenite ($T > A_f = 358$ K) and the characteristics of the constitutive behavior should be similar to that shown in Fig. 3, but the critical stress should increase due to the increase of temperature. At a higher temperature $T = 112$°C (385 K), the critical stress became larger due to that higher stress was needed for martensitic transformation, and the hysteresis loop became much smaller because the contribution of martensite became less significant. It can be conjectured that if temperature is sufficiently high so that the no stress is able to induce martensitic transformation, the material would be composed of austenite and the behavior of the material would be determined by austenite.

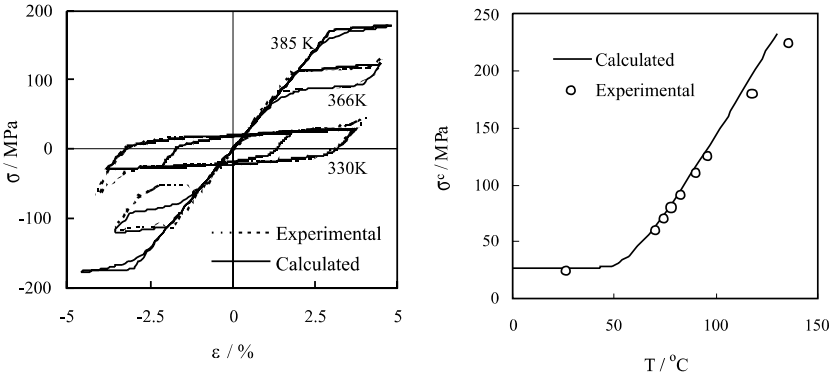

Fig. 4. Response of Au–47.5 at%Cd at different temperatures: (a) σ–ε curves at typical temperatures and (b) variation of critical stress vs. temperature.

Fig. 4(b) shows the temperature dependence of the critical stress. It can be seen that at lower temperature the critical stress almost keeps constant, while at higher temperature the increase of critical stress is almost linearly proportional to the increase of temperature. It is known from the previous discussion that at lower temperature the behavior of the SMA is mainly determined by the elastoplastic property of martensite. With the increase of temperature the volume fraction of austenite increases, the contribution of austenite to overall stress increases and the critical stress of the material, therefore, increases.

5. Analysis of the pseudoelastic behavior of Cu–Al–Zn–Mn SMA polycrystal

Sittner et al. (1995) and Sittner and Takuda (1995) systematically investigated the pseudoelastic behavior of Cu–Al–Zn–Mn SMA polycrystal at temperature $T = A_f + 25$ K. Thin-walled specimens with $d_{ext} = 8$ mm and $d_{int} = 5$ mm were used for the combined tension–torsion tests. The specimens were finally heat treated at 873 K for two hours and quenched in ice water. The measured grain size of the material was less than 120 μm in diameter. The transformation temperatures was determined by electric resistivity measurement as $M_f = 223$ K, $M_s = 239$ K, $A_s = 248$ K and $A_f = 260$ K. The experiment was performed in a stress or strain controlled mode. The shear strain and stress were calculated with (Sittner et al., 1995)

$$\gamma = \frac{d_{ext}\theta}{2l}, \quad \tau = \frac{16Md_{ext}}{\pi(d_{ext}^4 - d_{int}^4)} \tag{40}$$

where θ denotes the torsion angle in length l and M is the measured torque. It can be seen that if plastic deformation occurred, Eq. (40) might overestimate the shear strain and shear stress. An important phenomenon reported was that the equivalent stress and strain did not obey von Mises equivalent rule (Sittner et al., 1995). In the case of combined tensile–torsional loading the equivalent stress and strain were defined, by introducing factors C^S and C^E (Sittner et al., 1995), as

$$\sigma_{eq} = \sqrt{\sigma^2 + (C^S\tau)^2}, \quad \varepsilon_{eq} = \sqrt{\varepsilon^2 + (\gamma/C^E)^2}, \tag{41}$$

in which C^S was determined by the ratio of tensile and torsional yield stress, and C^E by the ratio of torsional and tensile yield strain. This phenomenon can be described by a proper definition of **P** (see Eq. (9)). First part of Eq. (9) can be expressed in the following matrix form by setting the sequence of plastic strain components as $(e^p_{11}, e^p_{22}, e^p_{33}, e^p_{12}, e^p_{13}, e^p_{21}, e^p_{23}, e^p_{31}, e^p_{32})$,

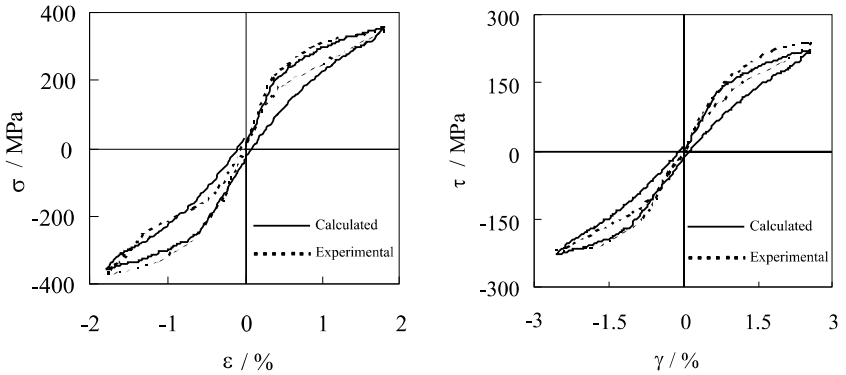

Fig. 5. Uniaxial stress–strain curves of Cu–Al–Zn–Mn SMA polycrystal, strain control, 285 K (a) symmetrical tension – compression and (b) symmetrical torsion.

$$[P] = \mathrm{diag}(1,1,1,k^2,k^2,k^2,k^2,k^2,k^2), \tag{42}$$

and it is easily found that the proposed model reduces to the initially isotropic case if $k^2 = 1$.

Since the experiments were performed at a constant temperature (Sittner et al., 1995; Sittner and Takuda, 1995), the effect of temperature on the material properties and the temperature induced phase-transformation strain $\mathbf{e}^{\mathrm{T}}$ (see Eq. (16)) would not be considered in the corresponding analysis. In Eqs. (7) and (11), $n = 3$ was also chosen to satisfy the requirements of both the accuracy and the efficiency in the analysis (Valanis and Fan, 1983), and $f(z) = 1$ was assumed as the experimental results did not show distinct isotropic hardening. Young's modulus and elastic shear modulus of austenite were measured as $E^0_{\mathrm{A}} = 53$ GPa and $G^0_{\mathrm{A}} = 19.5$ GPa (Sittner et al., 1995), and the other material constants were determined as follows

$$E^0_{\mathrm{M}}, G^0_{\mathrm{M}} = (16.2, 6.0)\ \mathrm{GPa}, \quad A_{\mathrm{a}}, B_{\mathrm{a}}, A_{\mathrm{m}}, B_{\mathrm{m}} = 0.028, 0.83, 0.035, 2.4$$
$$C^0_{1,2,3} = (550,\ 24, 1.1)\ \mathrm{GPa}, \quad \alpha_{1,2,3} = 10\,000, 420, 35, \ \ k^2 = 0.7$$

Fig. 5 shows the pseudoelastic behavior of the Cu–Al–Zn–Mn SMA polycrystal subjected to uniaxial forward and reverse straining. It can be seen that the basic characteristics of the pseudoelastic behavior of the material are satisfactorily replicated. Experimental observation (Sittner et al., 1995; Sittner and Takuda, 1995) showed that there existed small residual strain after unloading, which might be attributed to: (1) plastic deformation may also occurred to austenite, or (2) the reverse martensitic transformation may not be complete. The latter can be described with the proposed model without difficult, and the former can also be described by simply giving austenite elastoplastic property. Since the residual strain was very small, we tend to ignore it or equivalently describe it with the proposed model in order to reduce complexity.

The response of the SMA polycrystal subjected to non proportional strain along a square path in an ε–γ plane is shown in Fig. 6. The four vertexes of the square were $(0,0)$, $(0,0.0264)$, $(0.0178,0.0264)$, $(0.0178,0)$ in sequence. Both the experimental and the calculated results showed that the stress did not vanish when strain returned to the origin, which also implied the existence of residual strain after unloading. The error between the calculated and experimental results may partly be attributed to difference between the controlled strain paths. In calculation an ideal square strain path in ε–γ plane was used, while in the experiment (Sittner et al., 1995) an invariant value of shear strain was defined (see Eq. (39)) and used to control the experiment. Comparison showed that there was a distinct difference between the paths used in the analysis and used in the experiment. It should also be noted that there were marked differences between the coef-

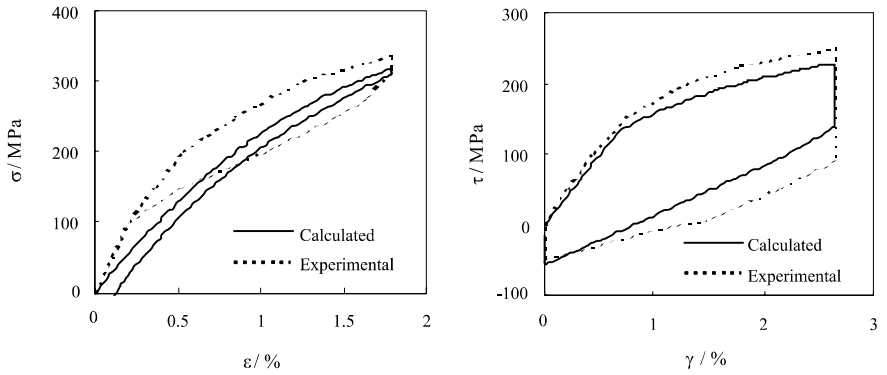

Fig. 6. Response of Cu–Al–Zn–Mn SMA polycrystal subjected to combined biaxial strain along a square path, $T = 285$ K: (a) tensile response and (b) torsional response.

ficients $C^S = \sigma^F/\tau^F$ (or $C^E = \gamma^F/\varepsilon^F$) obtained in different experiments (Sittner et al., 1995), but in the analysis, the material parameters kept unified throughout all the calculation.

The response of the SMA polycrystal subjected to nonproportional stress along a square path in a σ–τ plane is shown in Fig. 7. The four vertexes of the square were (0, 0), (250 MPa, 0), (250 MPa, 200 MPa), (0, 200 MPa) in sequence. Fig. 7(a) and (b) show respectively the tensile and torsional responses. Analysis showed that during the stress cycle, the material endured severe plastic deformation, but it almost recovered after unloading. In Fig. 7(a) and (b) the end point of stress and the corresponding strain were expressed with a small circle, which showed that the residual strain almost vanished.

Fig. 8 shows the response of the SMA polycrystal subjected to nonproportional stress along a triangular path in a σ–τ plane. The three vertexes of the triangle were (0, 0), (0, 260 MPa), (380 MPa, 0) in sequence. It was observed in experiment that, on one hand, the strain in a nonproportional stress loop was reversible, and on the other hand, the equivalent stress–strain loop corresponded well to the uniaxial pseudoelastic loop (Sittner et al., 1995; Sittner and Takuda, 1995). Both the two characteristics were satisfactorily replicated in the analysis. The small circles in Fig. 8(a) and (b) also represent the stress and strain after complete unloading, which shows that the residual strain almost completely recovered. The calculated

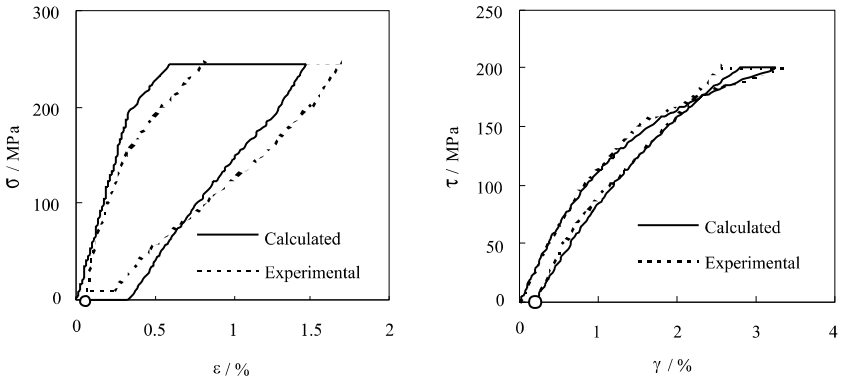

Fig. 7. Response of Cu–Al–Zn–Mn SMA polycrystals subjected to combined biaxial stress along a square path, $T = 285$ K: (a) tensile response and (b) torsional response.

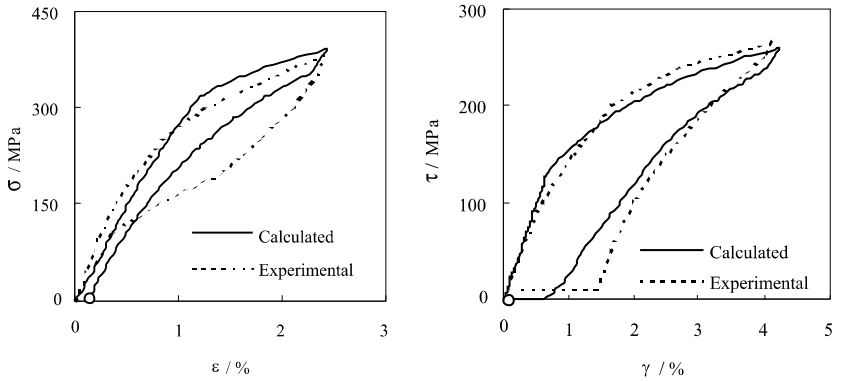

Fig. 8. Response of Cu–Al–Zn–Mn SMA polycrystal subjected to combined biaxial stress along a triangular path, $T = 285$ K: (a) tensile response and (b) torsional response.

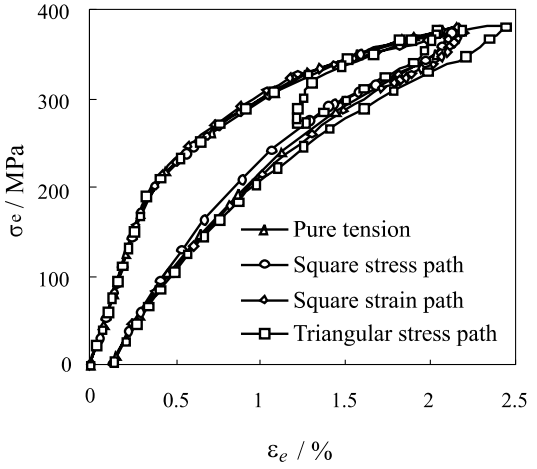

Fig. 9. Equivalent stress–strain relation along different loading paths.

equivalent stress–strain loop was shown in Fig. 9, which was almost identical to that under tensile loading and unloading.

Sittner et al. (1995) observed that the equivalent stress–strain loops corresponding to different non-proportional loading and unloading were well consistent with the uniaxial pseudoelastic loop. Substituting the definition of **P** (see Eq. (40)) into Eq. (9) and noticing the result in Eq. (15), the equivalent strain and stress in biaxial tension–torsion case can be obtained as

$$\varepsilon_{\mathrm{eq}} = \sqrt{\varepsilon^2 + k^2\gamma^2/3}, \quad \sigma_{\mathrm{eq}} = \sqrt{\sigma^2 + 3k^2\tau^2}. \tag{43}$$

Fig. 9 shows the σ_{eq}–$\varepsilon_{\mathrm{eq}}$ curves corresponding to the above four different loading paths in a biaxial tension–torsion stress or strain plane. Comparison showed that the σ_{eq}–$\varepsilon_{\mathrm{eq}}$ curves corresponding to non-proportional stress or strain paths are similar to tensile σ–ε curve. This implied that the pseudoealstic behavior of the SMA polycrystal under nonproportional loading can be characterized by the equivalent stress–strain relation obtained from uniaxial or proportional experiment (Sittner et al., 1995). It can be seen

from the curve corresponding to triangular stress path (see Fig. 9) that there were a small additional unloading–reloading and the corresponding reverse/forward martensitic transformation in this process, which resulted in some additional plastic strain. But the strain also recovered after completely unloading. This phenomenon was identical to the experimental observation (Sittner and Takuda, 1995).

6. Conclusions and discussions

A two-phase constitutive model was proposed for polycrystalline SMAs based on that a SMA is dynamically composed of austenite and martensite, and the overall constitutive behavior of the SMA is the dynamic combination of the individual behavior of each of the two phases. Within the interested ranges of stress and temperature, the behavior of austenite was assumed linearly elastic while that of martensite elastoplastic. Initial anisotropy of SMAs could be taken into account by introducing a forth order material property tensor **P**. The corresponding numerical algorithms for both strain- and stress-controlled process were proposed. The main characteristics of SMAs such as ferroelasticity, SME and pseudoelasticity can be described with the proposed model.

The ferroelasticity, pseudoelasticity and SME of SMA Au–47.5 at.%Cd subjected to uniaxial reversed loading at constant or varying temperature were successfully replicated. The pseudoelasticity of Cu–Al–Zn–Mn SMA polycrystal subjected to proportional and nonproportional complex stress and strain histories were analyzed and compared with the experimental results. The comparison between the calculated and experimental results show satisfactory agreement, and the validity of the proposed constitutive model was well demonstrated.

In the proposed two-phase constitutive model, the strains in the two phases of a SMA were assumed identical to the overall strain in the SMA, while the overall stress in the SMA was the sum of the contributions of the two phases. The complicated constitutive behavior of a polycrystalline SMA is separated into the simple constitutive behavior of its two phases, which provides a simple but comprehensive description for the constitutive behavior of SMAs. It is known that given a strain the stress response of a martensite is much lower than austenite, and that of a SMA usually lies between those of the two phases. The responses of both martensite and austenite can be determined individually under some specific thermomechanical loading conditions when the SMA is mainly composed of a single phase. If Reuss assumption were used for the analysis, i.e., the stress in the two phases of a SMA were assumed identical to the overall stress in the SMA. It can easily be found that the stress in martensite may exceed its load-bearing capability unless some residual stress was introduced, which needs additional analysis and may increase the complexity of the constitutive model. It has been observed that there may exist distinct microstructures inside the grains of some polycrystalline materials during stress-induced martensitic transformation (Siredey et al., 1999), which may give possibility to develop a microstructure-based two-phase constitutive model.

Martensite occurs in different variants, the number of which depends on the special type of the SMA under consideration. The plastic deformation of martensite is the macroscopic counterpart of the stress induced transformation between the variants. If many variants involved in a plastic deformation process, additional reorientation hardening/softening (Sun and Hwang, 1993) can be considered by introducing kinematic hardening terms to obtain a more realistic description.

It should be noted that plastic flow may also take place in austenite when the applied stress is sufficiently large. Although this kind of phenomenon was beyond the discussion in this paper, it can, however, be considered in the proposed constitutive framework by assuming that austenite is also elastoplastic. The decrease of the critical stress with the increase of temperature at lower temperature can also be described by simply assuming the decrease of $g_M(T)$ and $g_A(T)$ (see Eqs. (24) and (25)) with the increase of temperature, and the "V" shape of the relation between critical stress and temperature (Sun and Hwang, 1993) can thus be replicated.

Acknowledgements

The authors fully Acknowledge NSFC and the Education Ministry of China for their financial support.

References

Achenbach, M., Atanackovic, T., Muller, I., 1986. A model for memory alloys in plane strains. Int. J. Solids Struct. 22 (2), 171–193.
Auricchio, F., Taylor, R.L., Lubliner, J., 1997. Shape-memory alloys: macromodelling and numerical simulations of the superelastic behavior. Comp. Meth. Appl. Mech. Engng. 146 (3–4), 281–312.
Boyd, J.G., 1994. Thermomechanical response of shape memory composites. J. Intell. Mater. Syst. Struct. 5, 333–346.
Falk, F., 1980. Model free-energy, mechanics, and thermodynamics of shape memory alloys. Acta Metallurgica 23 (12), 1773–1780.
Fischer, F.D., Oberaigner, E.R., Tanaka, K., 1997. Micromechanical approach to constitutive equations for phase changing materials. Comput. Mater. Sci. 9 (1–2), 56–63.
Goo, B.C., Lexcellent, C., 1997. Micromechanics-based modeling of two-way memory effect of a single crystalline shape-memory alloy. Acta Materialia 45 (2), 727–737.
Graesser, E.J., Cozzarelli, F.A., 1991. Shape-memory alloys as new materials for a seismic isolation. J. Engng. Mech. 117 (11), 2590–2608.
Graesser, E.J., Cozzarelli, F.A., 1994. A proposed three-dimensional constitutive model for shape memory alloys. J. Intell. Mater. Syst. Struct. 5, 78–89.
Iwan, W.D., 1967. On a class of models for the yielding behavior of continuous and composite systems. J. Appl. Mech. 34, 612–627.
Fan, J., Peng, X., 1991. A physically based constitutive description for non proportional cyclic plasticity. J. Engng. Mat. Tech. 113, 254–262.
Levitas, V.I., 1995. Thermomechanics of martensitic phase transitions in elastoplastic materials. Mech. Res. Commun. 22 (1), 87–94.
Liang, C., Rogers, C.A., 1990. One-dimensional thermomechanical constitutive relations for shape memory materials. J. Intell. Mater. Syst. Struct. 1, 207–234.
Nakanishi, N., Mori, T., Miura, S., Murakami, Y., Kachi, S., 1973. Pseudoelasticity in Au–Cd thermoelastic martensite. Phil. Mag. 28, 277–292.
Patoor, E., Eberhardt, A., Berveiller, M., 1988. Thermomechanical behavior of shape memory alloys. Arch. Mech. 40, 775–794.
Peng, X., Ponter, A.R.S., 1994. A constitutive law for two-phase materials with experimental verification. Int. J. Solids Struct. 31 (8), 1099–1111.
Siredey, N., Patoor, E., Berveiller, M., Eberhardt, A., 1999. Constitutive equations for polycrystalline thermoelastic shape memory alloys. Part I. Intragranular interactions and behavior of the grain. Int. J. Solids Struct. 36 (28), 4289–4315.
Sittner, P., Hara, Y., Takuda, M., 1995. Experimental study on the thermoelastic martensitic transformation in shape memory alloy polycrystal induced by combined external forces. Metallurgical Mater. Trans. 26A, 2923–2935.
Sittner, P., Takuda, M., 1995. Reorientation in combined stress induced martensite. J. De Physique IV 5, C8-1003–C8-1008.
Sun, Q.P., Hwang, K.C, 1993. Micromechanics modeling for the constitutive behavior of polycrystalline shape memory alloys. J. Mech. Phys. Solids 41, 1–33.
Tanaka, K., Kobayashi, S., Sato, Y., 1986. Thermomechanics of transformation pseudoelasticity and shape memory effect in alloys. Int. J. Plasticity 2, 59–72.
Tanaka, K., 1986. Thermalmechanical sketch of shape memory effect – one-dimensional tensile behavior. Res. Mechanica 18 (3), 251–263.
Valanis, K.C., Fan, J., 1983. Endochronic analysis of cyclic elastoplastic strain fields in a notched plate. J. Appl. Mech. 50, 789–793.